Nonlinear Optical Effect of Interlayer Charge

Transfer in a van der Waals Heterostructure

Peng Yao, †,‡ Dawei He,† Peymon Zereshki,‡ Yongsheng Wang,*,† and Hui

 $7hao^{*,\ddagger}$

†Key Laboratory of Luminescence and Optical Information, Ministry of Education,

Institute of Optoelectronic Technology, Beijing Jiaotong University, Beijing 100044, China

‡Department of Physics and Astronomy, The University of Kansas, Lawrence, Kansas

66045, United States

E-mail: yshwang@bjtu.edu.cn; huizhao@ku.edu

Phone: 1-785-864-1938

Abstract

The recently discovered two-dimensional materials offer a new route to fabricating

multilayer heterostructures. Interlayer charge transfer is a key process in such het-

erostructures as it can enable emergent optoelectronic properties. Efficient interlayer

charge transfer in van der Waals heterostructures has been observed by femtosecond

transient absorption and steady-state optical spectroscopy measurements, based on

measuring the interlayer carrier distribution. Here we show that a second harmonic

generation process allows direct probe of the electric field induced by the charge trans-

fer. An ultrashort laser pulse was used to excite electrons and holes in a MoS₂/WS₂

heterostructure. The separation of the electrons and holes to the two monolayers gener-

ates an electric field, which enables generation of the second harmonic of an incident a

fundamental pulse. We further studied the time evolution of this electric field by mea-

suring the second harmonic signal as a function of the time delay between the pump

1

and the fundamental pulses. The result agrees well with the dynamics revealed by a transient absorption measurement. These results provide direct evidence of interlayer charge transfer, demonstrate a new method of studying charge transfer and induced electric fields in two-dimensional materials, and illustrate potential applications of van der Waals heterostructures as tunable nonlinear optical materials.

KEYWORDS: second-harmonic generation, van der Waals interface, transition metal dichalcogenide, electron transfer, transient absorption, two-dimensional material

The discovery of graphene¹ has created a fast-moving research field of two dimensional (2D) materials,² such as transition metal dichalcogenides (TMDs) and phosphorene. These atomically thin materials are attractive to both fundamental research and applications. One of the most intriguing aspects of 2D materials is that they provide a new route to fabricating multilayer heterostructures³ by combining several 2D materials with certain stacking orders via van der Waals interlayer interaction. Since lattice match is no longer a constrain, a large number of materials can be combined; hence, this approach can potential produce many new functional materials.⁴ One important process in van der Waals heterostructures is the interlayer charge transfer, which is the foundation for achieving emergent optoelectronic properties. Recently, this process has been studied by femtosecond transient absorption⁵⁻¹¹ and steady-state optical spectroscopy measurements.¹²⁻¹⁴ It was found that between two TMD monolayers that form a type-II band alignment, interlayer charge transfer occurs on an ultrashort time scale.^{5-9,12,15,16} Such observations are encouraging news for the development of van der Waals multilayers for electronic and optoelectronic technologies, and have stimulated significant discussions on the its physical mechanisms.¹⁷⁻²¹

So far, interlayer charge transfer has been studied only with experimental techniques based on detection of the carrier population. Here we show that a second harmonic generation (SHG) process allows direct probe of charge transfer by sensing the electric field produced by the charge separation. Using a MoS₂/WS₂ heterostructure as a model system, we show that

the separation of the photoexcited electrons and holes to the two monolayers generates an electric field, which is directly sensed by SHG of a fundamental pulse. These results provide a direct evidence of interlayer charge transfer, demonstrate a new method to study charge transfer and induced electric fields in 2D materials, and illustrate potential applications of van der Waals heterostructures as tunable nonlinear optical materials.

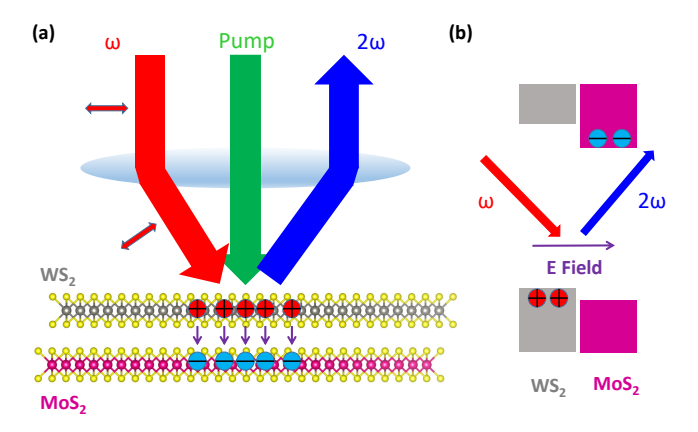


Figure 1: (a) Schematics of field-induced second harmonic generation: A pump pulse injects electrons and holes in a WS_2/MoS_2 heterostructure. Separation of the charge carriers generates an electric field, which is sensed by the second harmonic of an incident fundamental pulse (ω). (b) Band alignment of WS_2/MoS_2 and expected charge separation.

The experimental scheme of this study is shown in Figure 1. A pump pulse [the green arrow in (a)] injects electrons (-) and holes (+) in a WS₂/MoS₂ heterostructure. Because the conduction band minimum and the valence band maximum reside in the MoS₂ and WS₂ layers, respectively [as schematically shown in Figure 1(b)], the electrons and holes populate in these two layers, respectively. The charge separation results in an electric field pointing from WS₂ to MoS₂. To probe this field, a fundamental pulse (ω) is incident to the lens off-center. The oblique incidence (at about 12°) to the sample is essential for observing the effect, as it provides a component of the optical field along the direction of the space-charge field. The second harmonic (2ω) was collected in the reflection geometry with the same lens and was measured by a spectrometer equipped with a thermoelectrically cooled camera.

The inset of Figure 2 shows an optical microscope image of the WS_2/MoS_2 heterostructure sample, which was fabricated by standard exfoliation and dry transfer procedures.²² First,

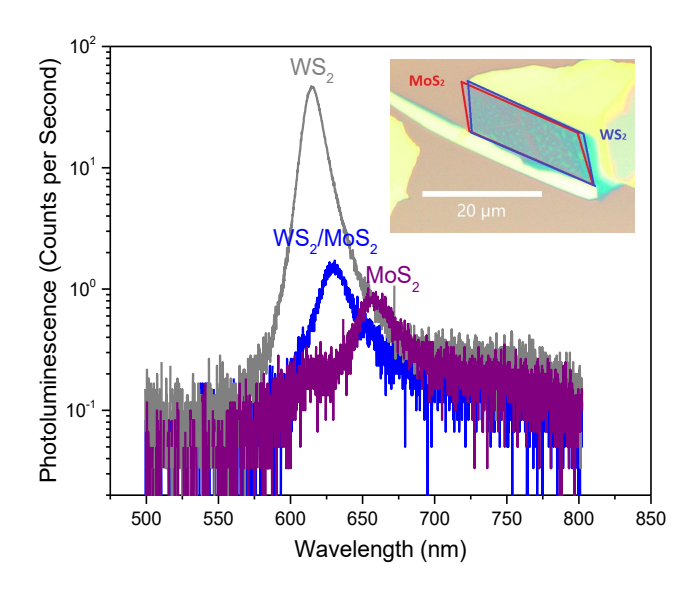


Figure 2: Photoluminescence spectra of the WS_2/MoS_2 heterostructure sample and two individual monolayer samples. The inset shows an optical microscope image of the heterostructure sample.

flakes of WS₂ and MoS₂ were exfoliated from their respective bulk crystals (acquired from 2D Semiconductors) to polydimethylsiloxane (PDMS) substrates. The green channel contrast under an optical microscope was used to initially identify the monolayer regions. ²³ A MoS₂ monolayer was transferred onto a Si/SiO₂ (90 nm) substrate, and annealed at 200°C in a H₂/Ar environment for 2 hours. Next, a WS₂ monolayer flake was transferred on top of the MoS₂ flake under a long-working-distance microscope. The heterostructure was annealed again under the same conditions.

The sample was first characterized by photoluminescence (PL) spectroscopy. The blue curve in Figure 2 shows a PL spectrum of the heterostructure obtained under the excitation of a 405-nm continuous-wave laser with a power of 1 μ W with the sample at room temperature. For comparison, monolayer flakes of MoS₂ and WS₂ that were fabricated together with the heterostructure sample were also measured under the same conditions, as shown by the purple and gray curves in Figure 2. The PL yield and peak position observed are consistent with previously results, confirming their monolayer thickness.²² The PL from the heterostructure is significantly lower than the corresponding monolayers. Such pronounced PL quenching has

been observed in TMD heterostructure and is indicative of the efficient charge transfer, which separates electrons and holes to different layers and thus suppress their recombination. ^{5–14}

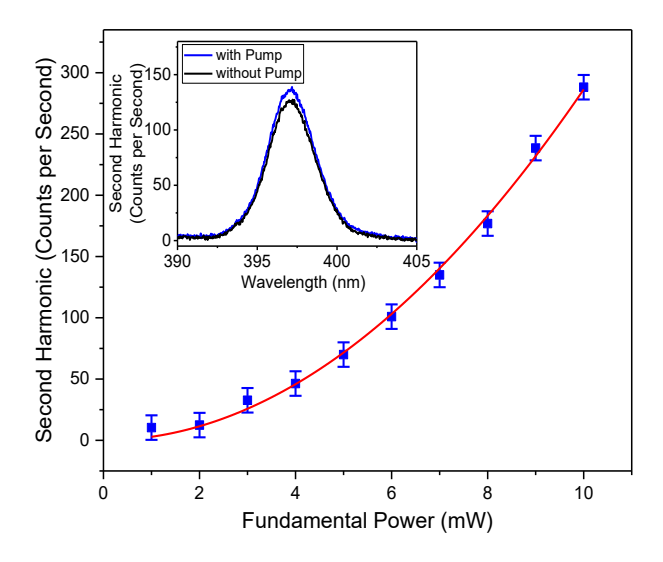


Figure 3: Second harmonic power as a function of the fundamental power. The red curve shows a quadratic fit. The inset shows the second harmonic spectra with and without the pump, respectively.

In the SHG measurement, a 795-nm and 100-fs fundamental pulse obtained from a 80-MHz mode-locked Ti:sapphire oscillator was focused to the sample. Its second harmonic at 397.5 nm was detected by a spectrometer. The black curve in the inset of Figure 3 shows the second harmonic spectrum measured with a 7-mW pump power, confirming the SHG origin of the signal. This is just the regular SHG process²⁴ that has been widely observed in 2D TMDs²⁵⁻²⁹ and their heterostructures,³⁰ where the second-order polarization, originated from the second-order nonlinear susceptibility of the sample, results in radiation at the double frequency of the fundamental. Next, we used a 600-nm pump pulse that arrives about 5 ps before the fundamental pulse to excite the sample. The electrons and holes excited are expected to separate, as illustrated in Figure 1. The resulted space-charge field is expected to induce an additional SHG process through a process known as the field-induced SHG.^{31,32} By measuring the second harmonic spectrum under the same conditions, we found that the second harmonic intensity is increased, as shown in the inset of Figure 3. The change is small, but repeatable as we verified by taking many back-to-back measurements of the

second harmonic spectra with and without the presence of the pump beam. As a further confirmation, we studied the pump-power dependence of the SHG. As shown in the main panel of Figure 3, the second harmonic power shows a quadratic dependence on fundamental power (the red curve), as expected.

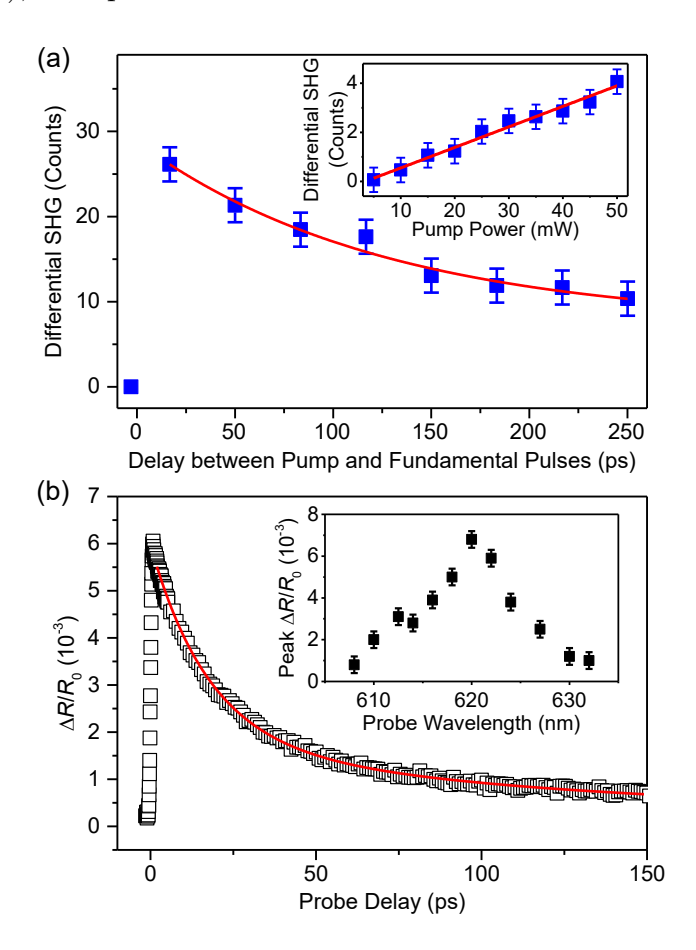


Figure 4: (a) Differential second harmonic signal as a function of the time delay between the pump and the fundamental pulses. The red curve is an exponential fit with a time constant of 125 ps, indicating the lifetime of the electric field. The inset shows the differential second harmonic signal is proportional to the pump power. (b) Differential reflection signal of a 620-nm probe measured with a 400-nm pump. The red curve is a bi-exponential fit with two time constants of 17 and 110 ps, respectively. The inset shows the probe-wavelength dependence of the differential reflection signal.

We next used the SHG to probe the space-charge field by measuring the differential SHG signal, which is defined as the difference between the second harmonic intensities with and without the presence of this field. To measure this quantity for a certain time delay between the pump and the fundamental pulses, we acquire a pair of second harmonic spectra with

the delays of that value and -3 ps, respectively. The latter spectrum detects the regular SHG without the field, since the pump arrives at the sample after the fundamental pulse in this case. The difference between these two spectra thus measures the field-induced SHG corresponding to the space-charge field at that time delay. We first established the relation between the differential SHG and the strength of the space-charge field by measuring this quantity (with a delay of 15 ps) as a function of the pump power. The results are shown in the inset of Figure 4(a). Clearly, the differential SHG is proportional to the pump power. Since the space-charge field is proportional to the injected carrier density, which is in turn proportional to the pump power, this result shows that the differential SHG is proportional to the space-charge field. To understand this result, we note that the measured second harmonic intensity is the result of two fields, the regular SHG of the sample (A_0) and the field-induced SHG (A_F) , $I = (c\epsilon_0/2)(A_0 + A_F)^2 = (c\epsilon_0/2)(A_0A_0^* + A_FA_F^* + A_0A_F^* + A_FA_0^*) = (c\epsilon_0/2)(A_0A_0^* + A_FA_F^* + A_0A_F^* + A_0A_F^* + A_0A_F^*)$ $I_0 + I_F + (c\epsilon_0/2)(A_0A_F^* + A_FA_0^*)$. Since the field-induced SHG is much weaker than the regular SHG (see the inset of Figure 3), we can ignore I_F and the regular SHG actually act as a local amplifier for a homodyne coherent detection.³³ Hence, the differential SHG $\Delta I = I - I_0 \approx (c\epsilon_0/2)(A_0A_F^* + A_FA_0^*)$. Since A_F is proportional to the field-induced secondorder susceptibility, the result shown in the inset of Figure 4 proves that the field-induced susceptibility is proportional to the space charge field.

To probe the time evolution of the space-charge field, we measured the differential SHG as a function of the time delay between the fundamental and the pump pulses, as summarized by the blue squares in the main panel of Figure 4(a). By fitting the data with a single-exponential function, we found a decay time constant of 125 ± 30 ps, as indicated by the red curve in Figure 4(a). The result indicates that the space-charge field created by the charge transfer has a lifetime of about 125 ps. This can be attributed to the recombination of electrons and holes.

To further confirm this interpretation, we also preformed a transient absorption measurement on the same sample.³⁴ We used a 400-nm pump pulse to inject electrons and holes.

After the charge transfer process, electrons and holes populate the MoS₂ and WS₂ layers, respectively. We used a 620-nm probe to monitor the population of the holes in WS₂ by measuring its differential reflection, defined as $\Delta R/R_0 = (R-R_0)/R_0$, where R and R_0 are the reflectance of the sample with and without the pump excitation, respectively. The result is shown in Figure 4(b). We found that the decay of $\Delta R/R_0$ is a bi-exponential process [the red curve in Figure 4(b)], with two time constants of 17 and 110 ps, respectively. The long time constant is reasonably consistent with the lifetime of the space-charge field deduced from the time-dependent differential SHG measurement. The short time constant is similar to exciton lifetime in monolayer WS₂. ²² It could be attributed to the recombination of excitoins in WS₂ after their generation in the regions of sample with poor interface and thus inefficient charge transfer. Furthermore, we confirm that the 620-nm probe senses the exciton resonance of WS₂ by measuring the peak $\Delta R/R_0$ as a function of the probe wavelength. As shown in the inset of Figure 4(b), the spectrum of the signal agrees well with the A-exciton resonance of WS₂.

Finally, we provide an order-of-magnitude estimation of the strength of the SHG induced by the space-charge field, by comparing it with the regular SHG of TMDs. From the spectra shown in the inset of Figure 3, $\Delta I/I_0$ is about 0.1. Based on the above analysis of the homodyne detection, this indicates that the field-induced susceptibility is about 10% of that of the regular susceptibility of the sample. To estimate the magnitude of the electric field in this measurement, we treat the heterostructure as a parallel-plate capacitor. The pump power of 50 μ W corresponding to a peak fluence of 0.8 μ J cm⁻². According to the absorption coefficient ³⁵ of about 3×10^7 m⁻¹, this pulse injects a peak carrier density of 2×10^{11} cm⁻². Assuming all the injected electrons and holes transfer, the peak charge density (at the center of laser spot) in WS₂ is 3.2×10^{-4} C m², leaving the same density of negative charges in MoS₂. This gives an electric field on the order of 10^6 V m⁻¹, using an average dielectric constant of about 7. Since the second-order nonlinear susceptibilities of monolayer TMDs ^{26–29} are on the order of 10^{-9} , we conclusion that a space-charge field on the order of 10^6 V m⁻¹ induces

a susceptibility on the order of 10^{-10} .

In summary, we have observed second-harmonic generation induced by the electric field due to interlayer charge transfer in a TMD heterostructure. The observation provides unambiguous evidence of interlayer charge transfer in van der Waals heterostructures, offers a new methods to study the charge transfer with high temporal resolution, and suggest the possibility of new optical devices based on 2D heterostructures with nonlinear optical responses controllable by interlayer charge transfer.

Acknowledgments

We are grateful for the financial support of the National Key R&D Program of China (2016YFA0202302), the National Natural Science Foundation of China (61527817, 61875236), National Science Foundation of USA (DMR-1505852) and KU Research GO Fund.

References

- (1) Novoselov, K. S.; Geim, A. K.; Morozov, S. V.; Jiang, D.; Zhang, Y.; Dubonos, S. V.; Grigorieva, I. V.; Firsov, A. A. Electric Field Effect in Atomically Thin Carbon Films. Science 2004, 306, 666–669.
- (2) Gibney, E. The Super Materials that Could Trump Graphene. *Nature* **2015**, *522*, 274–276.
- (3) Geim, A. K.; Grigorieva, I. V. Van der Waals Heterostructures. *Nature* **2013**, 499, 419–425.
- (4) Novoselov, K. S.; Mishchenko, A.; Carvalho, A.; Neto, A. H. C. 2D Materials and van der Waals Heterostructures. *Science* **2016**, *353*, 461.
- (5) Hong, X.; Kim, J.; Shi, S. F.; Zhang, Y.; Jin, C.; Sun, Y.; Tongay, S.; Wu, J.; Zhang, Y.;

- Wang, F. Ultrafast Charge Transfer in Atomically Thin MoS₂/WS₂ Heterostructures. Nat. Nanotechnol. **2014**, *9*, 682–686.
- (6) Ceballos, F.; Bellus, M. Z.; Chiu, H. Y.; Zhao, H. Ultrafast Charge Separation and Indirect Exciton Formation in a MoS₂-MoSe₂ van der Waals Heterostructure. ACS Nano 2014, 8, 12717–12724.
- (7) Ceballos, F.; Bellus, M. Z.; Chiu, H. Y.; Zhao, H. Probing Charge Transfer Excitons in a MoSe₂-WS₂ van der Waals Heterostructure. *Nanoscale* **2015**, *7*, 17523–17528.
- (8) Peng, B.; Yu, G.; Liu, X.; Liu, B.; Liang, X.; Bi, L.; Deng, L.; Sum, T. C.; Loh, K. P. Ultrafast Charge Transfer in MoS₂/WSe₂ P-N Heterojunction. 2D Mater. 2016, 3, 025020.
- (9) Zhu, H. M.; Wang, J.; Gong, Z. Z.; Kim, Y. D.; Hone, J.; Zhu, X. Y. Interfacial Charge Transfer Circumventing Momentum Mismatch at Two-Dimensional Van Der Waals Heterojunctions. *Nano Lett.* 2017, 17, 3591–3598.
- (10) Yuan, L.; Chung, T. F.; Kuc, A.; Wan, Y.; Xu, Y.; Chen, Y. P.; Heine, T.; Huang, L. B. Photocarrier Generation from Interlayer Charge-Transfer Transitions in WS₂-Graphene Heterostructures. *Sci. Adv.* **2018**, *4*, e1700324.
- (11) Wen, X. W. et al. Ultrafast Probes of Electron-Hole Transitions between Two Atomic Layers. *Nat. Commun.* **2018**, *9*, 1859.
- (12) Rigos, A. F.; Hill, H. M.; Li, Y. L.; Chernikov, A.; Heinz, T. F. Probing Interlayer Interactions in Transition Metal Dichalcogenide Heterostructures by Optical Spectroscopy: MoS₂/WS₂ and MoSe₂/WSe₂. Nano Lett. 2015, 15, 5033–5038.
- (13) Kozawa, D.; Carvalho, A.; Verzhbitskiy, I.; Giustiniano, F.; Miyauchi, Y.; Mouri, S.; Neto, A. H. C.; Matsuda, K.; Eda, G. Evidence for Fast Interlayer Energy Transfer in MoSe₂/WS₂ Heterostructures. *Nano Lett.* **2016**, *16*, 4087–4093.

- (14) Yang, B. W.; Molina, E.; Kim, J.; Barroso, D.; Lohmann, M.; Liu, Y. W.; Xu, Y. D.; Wu, R. Q.; Bartels, L.; Watanabe, K.; Taniguchi, T.; Shi, J. Effect of Distance on Photoluminescence Quenching and Proximity-Induced Spin-Orbit Coupling in Graphene/WS₂ Heterostructures. Nano Letters 2018, 18, 3580–3585.
- (15) Schaibley, J. R.; Rivera, P.; Yu, H. Y.; Seyler, K. L.; Yan, J. Q.; Mandrus, D. G.; Taniguchi, T.; Watanabe, K.; Yao, W.; Xu, X. D. Directional Interlayer Spin-Valley Transfer in Two-Dimensional Heterostructures. *Nat. Commun.* 2016, 7, 13747.
- (16) Ji, Z. H.; Hong, H.; Zhang, J.; Zhang, Q.; Huang, W.; Cao, T.; Qiao, R. X.; Liu, C.; Liang, J.; Jin, C. H.; Jiao, L. Y.; Shi, K. B.; Meng, S.; Liu, K. H. Robust Stacking-Independent Ultrafast Charge Transfer in MoS₂/WS₂ Bilayers. ACS Nano 2017, 11, 12020–12026.
- (17) Zhu, X.; Monahan, N. R.; Gong, Z.; Zhu, H.; Williams, K. W.; Nelson, C. A. Charge Transfer Excitons at van der Waals Interfaces. J. Am. Chem. Soc. 2015, 137, 8313– 8320.
- (18) Long, R.; Prezhdo, O. V. Quantum Coherence Facilitates Efficient Charge Separation at a MoS₂/MoSe₂ van der Waals Junction. *Nano Lett.* **2016**, *16*, 1996–2003.
- (19) Wang, H.; Bang, J.; Sun, Y. Y.; Liang, L. B.; West, D.; Meunier, V.; Zhang, S. B. The Role of Collective Motion in the Ultrafast Charge Transfer in van der Waals Heterostructures. *Nat. Commun.* 2016, 7, 11504.
- (20) Zheng, Q. J.; Saidi, W. A.; Xie, Y.; Lan, Z. G.; Prezhdo, O. V.; Petek, H.; Zhao, J. Phonon-Assisted Ultrafast Charge Transfer at van der Waals Heterostructure Interface. Nano Lett. 2017, 17, 6435–6442.
- (21) Wang, Y.; Wang, Z.; Yao, W.; Liu, G. B.; Yu, H. Y. Interlayer Coupling in Commensurate and Incommensurate Bilayer Structures of Transition-Metal Dichalcogenides. *Phys. Rev. B* **2017**, *95*, 115429.

- (22) Ceballos, F.; Zereshki, P.; Zhao, H. Separating Electrons and Holes by Monolayer Increments in van der Waals Heterostructures. *Phys. Rev. Mater.* **2017**, *1*, 044001.
- (23) Cui, Q.; Muniz, R. A.; Sipe, J. E.; Zhao, H. Strong and Anisotropic Third-Harmonic Generation in Monolayer and Multilayer ReS₂. *Phys. Rev. B* **2017**, *95*, 165406.
- (24) Boyd, R. W. Nonlinear Optics, 3rd ed.; Academy Press: San Diego, USA, 2008.
- (25) Kumar, N.; Najmaei, S.; Cui, Q.; Ceballos, F.; Ajayan, P. M.; Lou, J.; Zhao, H. Second Harmonic Microscopy of Monolayer MoS₂. *Phys. Rev. B* **2013**, *87*, 161403.
- (26) Malard, L. M.; Alencar, T. V.; Barboza, A. P. M.; Mak, K. F.; de Paula, A. M. Observation of Intense Second Harmonic Generation from MoS₂ Atomic Crystals. *Phys. Rev. B* 2013, 87, 201401.
- (27) Li, Y.; Rao, Y.; Mak, K. F.; You, Y.; Wang, S.; Dean, C. R.; Heinz, T. F. Probing Symmetry Properties of Few-Layer MoS₂ and h-BN by Optical Second-Harmonic Generation. *Nano Lett.* **2013**, *13*, 3329–3333.
- (28) Clark, D. J.; Senthilkumar, V.; Le, C. T.; Weerawarne, D. L.; Shim, B.; Jang, J. I.; Shim, J. H.; Cho, J.; Sim, Y.; Seong, M. J.; Rhim, S. H.; Freeman, A. J.; Chung, K. H.; Kim, Y. S. Strong Optical Nonlinearity of CVD-Grown MoS₂ Monolayer as Probed by Wavelength-Dependent Second-Harmonic Generation. *Phys. Rev. B* **2014**, *90*.
- (29) Seyler, K. L.; Schaibley, J. R.; Gong, P.; Rivera, P.; Jones, A. M.; Wu, S.; Yan, J.; Mandrus, D. G.; Yao, W.; Xu, X. Electrical Control of Second-Harmonic Generation in a WSe₂ Monolayer Transistor. *Nat. Nanotechnol.* 2015, 10, 407–411.
- (30) Hsu, W. T.; Zhao, Z. A.; Li, L. J.; Chen, C. H.; Chiu, M. H.; Chang, P. S.; Chou, Y. C.; Chang, W. H. Second Harmonic Generation from Artificially Stacked Transition Metal Dichalcogenide Twisted Bilayers. ACS Nano 2014, 8, 2951–2958.

- (31) Qi, J.; Yeganeh, M. S.; Koltover, I.; Yodh, A. G.; Theis, W. M. Depletion-electric-field-induced changes in second-harmonic generation from GaAs. *Phys. Rev. Lett.* **1993**, *71*, 633.
- (32) Aktsipetrov, O. A.; Fedyanin, A. A.; Golovkina, V. N.; Murzina, T. V. Optical second-harmonic generation induced by a DC electric field at the Si-SiO₂ interface. *Optics Lett.* **1994**, *19*, 1450.
- (33) Werake, L. K.; Zhao, H. Observation of second-harmonic generation induced by pure spin currents. *Nat. Phys.* **2010**, *6*, 875.
- (34) Ceballos, F.; Zhao, H. Ultrafast Laser Spectroscopy of Two-Dimensional Materials beyond Graphene. *Adv. Funct. Mater.* **2017**, *27*, 1604509.
- (35) Liu, H.-L.; Shen, C.-C.; Su, S.-H.; Hsu, C.-L.; Li, M.-Y.; Li, L.-J. Optical Properties of Monolayer Transition Metal Dichalcogenides Probed by Spectroscopic Ellipsometry. *Appl. Phys. Lett.* **2014**, *105*, 201905.